Supercritical CO_2 as heat transfer fluid: A review

Luisa F. Cabeza[a,*], Alvaro de Gracia[b], A. Inés Fernández[c], Mohammed M. Farid[d]

[a] GREA Innovació Concurrent, Universitat de Lleida, Lleida, Spain. Edifici CREA, Pere de Cabrera s/n, 25 001-Lleida, Spain

[b] Departament d'Enginyeria Mecànica, Universitat Rovira i Virgili, Av. Països Catalans 26, 43007, Tarragona, Spain.

[c] Department of Materials Science and Metallurgical Engineering, Universitat de Barcelona. Martí i Franquès, 1, 08028-Barcelona, Spain

[d] Department of Chemical and Materials Engineering, The University of Auckland, New Zealand

* Corresponding author: lcabeza@diei.udl.cat

Abstract

This paper presents a comprehensive review of all correlations and experimental studies available in the literature to determine the heat transfer coefficient of supercritical CO_2flowing in heat exchangers. The different applications in which it is used are also reviewed and discussed. The correlations obtained from extensive experimental measurements are presented for different geometries (horizontal, vertical and inclined tubes, closed-loop circular pipes, and mini-channels) and dimensions. The review shows that there is a lack of a unique universal correlation for each geometry, suggesting the need for more work in this area.

Keywords: supercritical CO_2; heat transfer fluid; heat exchanger; empirical correlation; cooling

Nomenclature

c_p	specific heat at constant pressure [J/kg·K]
$\overline{c_p}$	average specific heat at constant pressure [J/kg·K]
D	Inner diameter [m]
f	friction factor [-]
G	mass flux [kg/m^2·s]
Gr	Grasshof number [-]
g	gravity acceleration [m^2/s]
h	specific enthalpy [J/kg]

k	thermal conductivity [W/m·K]
L	tube length [m]
Nu	Nusselt number [-]
p	Pressure [Pa]
Pr	Prandtl number [-]
$\overline{\mathrm{Pr}}$	average Prandtl number [-]
q	heat flux from tube wall to fluid [W/m^2]
Re	Reynolds number [-]
Rr	channel relative roughness
T	Temperature [K]
Greek symbols	
α	heat transfer coefficient [W/m^2·K]
β	thermal expansion coefficient [1/K]
Δ	Increment
ε	channel roughness [m]
μ	dynamic viscosity [Pa·s]
ρ	density [kg/m^3]
Subscripts	
ac	Acceleration
b	at fluid bulk temperature
exp	experimental
f	at film temperature
in	Inlet
Iso	Isothermal
Out	Outlet
Pc	at pseudo-critical temperature
Pred	Predicted
W	at inner wall temperature

1. Introduction

Supercritical fluid is a fluid state where it is held at or above its critical temperature and critical pressure. Carbon dioxide behaves as a supercritical fluid above its critical temperature (304.25 K) and critical pressure (72.9 atm or 7.39 MPa), expanding to fill its container like a gas but with a density like that of a liquid (Figure 1). When fluids and gases are heated above their critical temperature and compressed above their critical pressure they enter a supercritical phase where some properties, such as solvent power, can be dramatically changed. Figure 2 shows in images how CO_2 goes through different phases from behaving as a sub-critical fluid to a supercritical fluid.

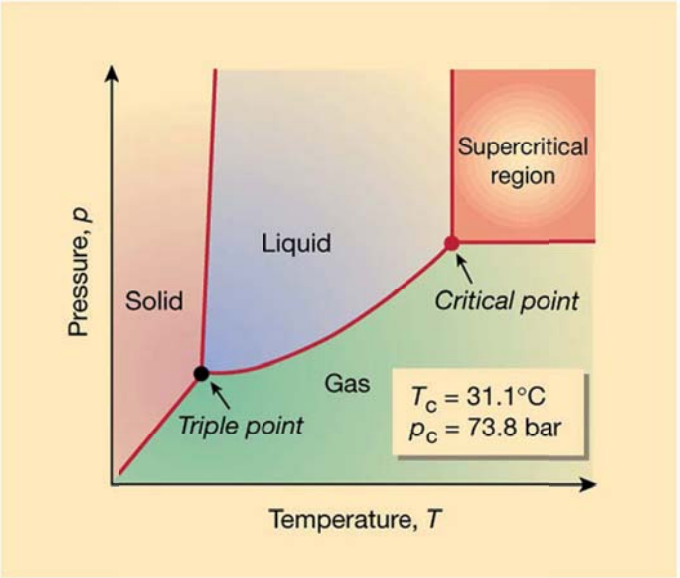

Figure 1. Supercritical CO2 p-T diagram [1]

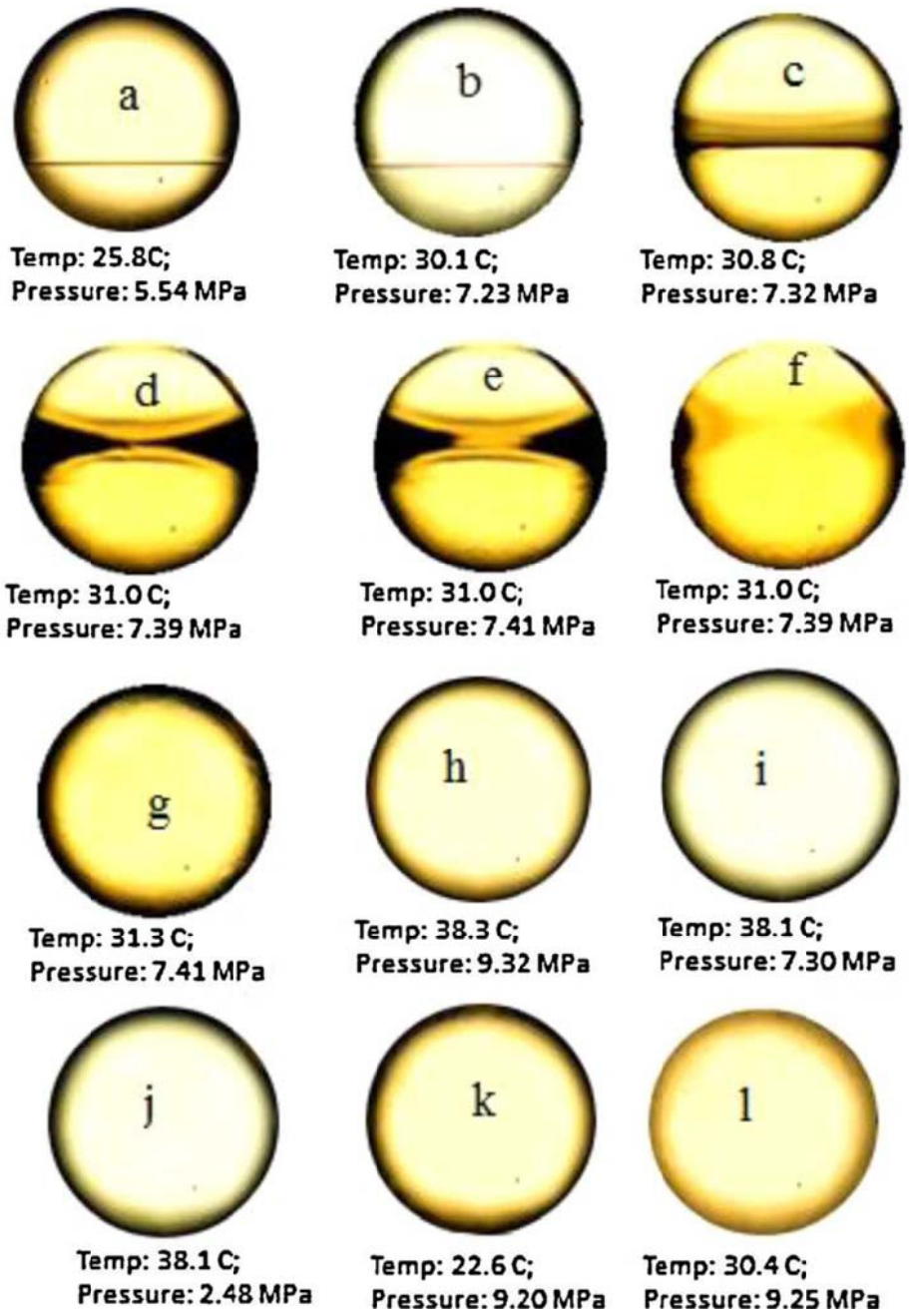

Figure 2. Transition of CO_2 through various phases. (a) sub-critical; (b)-(g) transition through critical point; (h) supercritical fluid; (i) between supercritical fluid and superheated vapour; (j) superheated vapour; (k) compressed fluid; and (l) between compressed fluid and supercritical fluid [2].

Okamoto et al. [3] in 2003 successfully visualized the variation of $scCO_2$ under forced convective heat transfer using schlieren and shadowgraph techniques as research towards the precise characterization of supercritical fluid behaviour. For example, Figure 3 presents scCO2 imaging by infrared laser and its translation to an instantaneous vector map and the average velocity distributions.

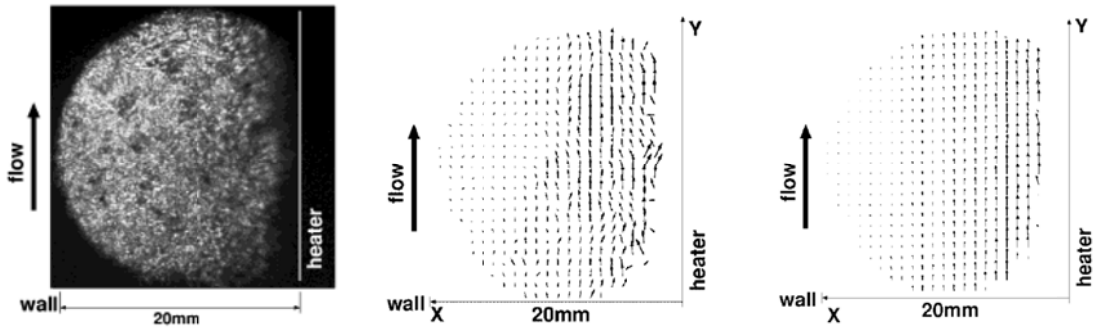

Figure 3. $scCO_2$ imaging [3]: (a) image captured by infrared laser and high-speed camera; (b) instantaneous vector map; (c) averaged velocity distributions.

Supercritical CO_2 is becoming an important commercial and industrial solvent due to its role in chemical extraction in addition to its low toxicity and being environmental friendly solvent. The relatively low temperature of the process and the stability of CO_2 also allow most compounds to be extracted with little damage or denaturing. In addition, the solubility of many extracted compounds in CO_2 varies with pressure, permitting selective extractions. $scCO_2$ has been used for fluid extraction in areas such as food science, pharmaceuticals, chemical residues, biofuels, and polymers [4].

The aim of this review is to summarize the literature on the use of $scCO_2$ as a heat transfer fluid (HTF), however its wider application of extraction will also be summarized in this review.

2. Applications of supercritical CO_2

A short summary of supercritical CO_2 applications is presented here. Supercritical carbon dioxide ($scCO_2$) offers an acceptable combination of pressure and temperature to achieve supercritical conditions. $scCO_2$ is not a good solvent for most materials, which are $scCO_2$-phobic. However, both silicone and fluoro-products may be regarded as CO_2-philic and, therefore, potentially more soluble; such products are used in magnetic media production, one of the first applications of $scCO_2$ studied [5].

Another application investigated was supercritical extraction in petroleum refining and petrochemistry [6]. According to this publication, the advantages of carbon dioxide as solvent include: non-explosiveness and incombustibility; chemical inertness; absence of toxic wastes; sufficiently low critical parameters (pressure and temperature); low polarity; availability and low cost; high extraction rate due to high diffusing power.

The food industry is always looking for the best separation technology to obtain natural compounds of high purity, healthy products of excellent quality with several industrial applications. The conventional extraction process for those compounds has some limitations regarding the solvent toxicity, flammability and wastefulness. Supercritical carbon dioxide is ideal for the food processing industry because of its non-flammable, non-toxic, non-polluting and recoverable characteristics [7,8]. Examples of applications in the food industry are extraction of cholesterol and other lipids from egg yolk; milk fat fractioning; extraction of lipids and cholesterol from meat and meat products; from fish; extraction of natural colourings from several foodstuffs (such as carrots, leaf protein concentrates, sweet potatoes, tomato paste waste and tomato skin, and rape grape skin); extraction, refining and fractioning of oils and vegetable fats; extraction and fractioning of natural flavourings; extraction of antioxidants; decaffeinating of coffee and tea; extraction of hop; and the alcoholisation of drinks.

$scCO_2$ is also used in separation processes [9]. For example, Semenova and Ohya [10] studied the fractionation of SC CO2/ethanol and scCO2/iso-octane mixtures using an asymmetric Kapton membrane. The investigators concluded that CO_2 transfer across was predominantly by convection rather than diffusion. At approximately the same time, Hsu and Tan [11] proposed the use of reverse osmosis membranes to fractionate water/ethanol mixtures in the presence of $scCO_2$. Under these conditions ethanol extraction is improved from 20 to 70%. The authors attributed the improved rejection to the formation of CO_2 and ethanol clusters.

The high volatility and low polarity of $scCO_2$ make it an interesting solvent partner with non-volatile and fairly polar ionic liquids (ILs) [12]. The different miscibility of $scCO_2$ and ILs lead to two-phase systems that have found application in several areas. The success of this two-phase system is based on solubility of $scCO_2$ in the IL, which is controlled by pressure, but insolubility of the IL in $scCO_2$. The solubility of $scCO_2$ in ILs also facilitates mass transfer processes by decreasing their viscosity.

$scCO_2$ has also been applied in fluid extraction in biotechnology [13]. Although $scCO_2$ is unfriendly, or even toxic, for some living cells and precludes direct fermentation in dense CO_2, it does not rule out other useful applications for *in situ* extraction of inhibitory fermentation products and fractional extraction of biomass constituents. In this application, the response of microorganisms to high pressure and temperature must be considered to assess possibility and effectiveness, as well as the economic aspects of the proposed processes. Similarly, growth of microalgae using CO_2 enriched air for biodiesel production in $scCO_2$ was studied, and it was found that the conversion of biodiesel produced from microalgae lipids was 35% higher than that achieved using lamb fat in a similar system [14].

Song et al. [15] recognized in 2006 that even though CO_2 is a greenhouse gas, it is much more environmentally benign than many of the existing solvents used in industries. Environment-friendly and energy-efficient processes can be designed by using CO_2 for separation, chemical reaction and materials synthesis based on the unique physical or chemical properties of CO_2. For example, supercritical CO_2 can be used either as a solvent for separation or as a medium for chemical reaction, or as both solvent and reactant.

$scCO_2$ has been also used in extrusion processes, for example in polymer foaming [16]. $scCO_2$ is soluble in molten polymers and acts as plasticizer and the dissolution of $scCO_2$ in polymers leads to a decrease its viscosity. Therefore, extrusion processes would benefit from the use of $scCO_2$ since the rationale of extrusion processes is to formulate, texture and shape molten polymers by forcing them through a die. Applications using $scCO_2$ in extrusion processes are foodstuffs (i.e. breakfast cereals and snack foods); foaming of polymers (i.e. polystyrene and polycarbonate); composites (such as clay-polymer nanocomposites); biopolymers and pharmaceutical applications (dispersion to a molecular level of a pharmaceutical ingredient in a polymeric matrix).

Supercritical CO_2 is considered as a promising alternative to volatile organic solvents currently used in certain industrial processes and products, however, the poor solubilizing power of CO_2 towards polar substances remains a significant barrier to applications. Employing effective surfactants which generate stable dispersions and water/CO_2 microemulsions is accepted as one way to improve the physico-chemical properties of CO_2 [17]. With compatible surfactants being developed, the applications of CO_2 as a green and easy to process solvent have received intensive interest. Studied applications in this field are synthesis of nanoparticles in w/c microemulsions and ionic liquid in $scCO_2$ microemulsions.

$scCO_2$ also has many unique properties and thus has great potential for advanced, green materials processing [1]. Applications cited are $scCO_2$ processing of 3D aerogels and of coatings; exfoliation and intercalation of layered materials (such as graphite, BN, MoS_2 and WS_2), even improving mechanical properties of the exfoliated of the layered material (silicate in a PET matrix); processing of powder materials for different applications (i.e. impregnating nanoparticles to support materials or preparation of hollow inorganic spheres).

A newer application is the used of $scCO_2$ as heat transfer fluid (HTF) in power cycles and CSP [18,19,20,21], solar collectors [22], or in carbon capture and storage (CCS) [23,24].The $scCO_2$ thermodynamic cycle was initially considered as a good substitute to the steam Rankine cycle in advanced nuclear reactors [25]. Its use was proposed for solar power applications [26] and fossil

fuel power applications [27]. To overcome the upper temperature limits of the ORC systems, Manente and Lazzaretto [19] proposed a new biomass to electricity conversion system, which is based on an externally fired supercritical CO_2 power cycle ($scCO_2$ cycle). The potential benefits in terms of system efficiency arise from the achievement of higher maximum cycle temperatures (around 550 °C) due to the elimination of the heat transfer medium (thermal oil) that is made possible by the direct heat transfer between the CO_2 as a working fluid in the power cycle and the combustion gases. Another advantage is the higher thermal efficiency of the closed Brayton cycle using $scCO_2$ compared to the Rankine cycle in this temperature range. Moreover, to improve the safety of the heat transport system of nuclear reactors and the cycle performances of their thermodynamic cycle, the supercritical gas Brayton cycle has been adopted as an alternative to the subcritical gas Brayton cycle [20]. In the supercritical gas Brayton cycle, the lowest cycle temperature and pressure, which are the inlet conditions of the main compressor, are located above but close to the critical point of the coolant. Thus, the working fluid behaves more like a liquid than a gas through the main compressor, resulting in significantly reduced compressor work, and consequently an increased cycle efficiency [28].

3. $scCO_2$ properties

The use of $scCO_2$ in cooling and power cycles requires a proper determination of the cooling heat transfer processes, which is an unsolved issue. As shown in Figure 4, the thermophysical properties of CO_2 change dramatically with temperature and pressure in the supercritical region [2,29,30]. For a given pressure, thermal conductivity, dynamic viscosity and density are strongly decreased with the increase in temperature. Moreover, the isobaric heat capacity presents a peak at critical point and pseudocritical temperatures which is reduced as the pressure increases. These heat capacity sharp peaks are similar to the ones obtained in phase change processes of mixtures used for thermal energy storage purposes [31,32], however, the dramatic decrease of density limits the potential of the sCO_2 to be used as storage media. These variations of the fluid make its heat transfer performance different from conventional fluids, especially in the determination of the convective heat transfer coefficient from a heat transfer surface, and the steady state supercritical natural circulation flows [33,34].

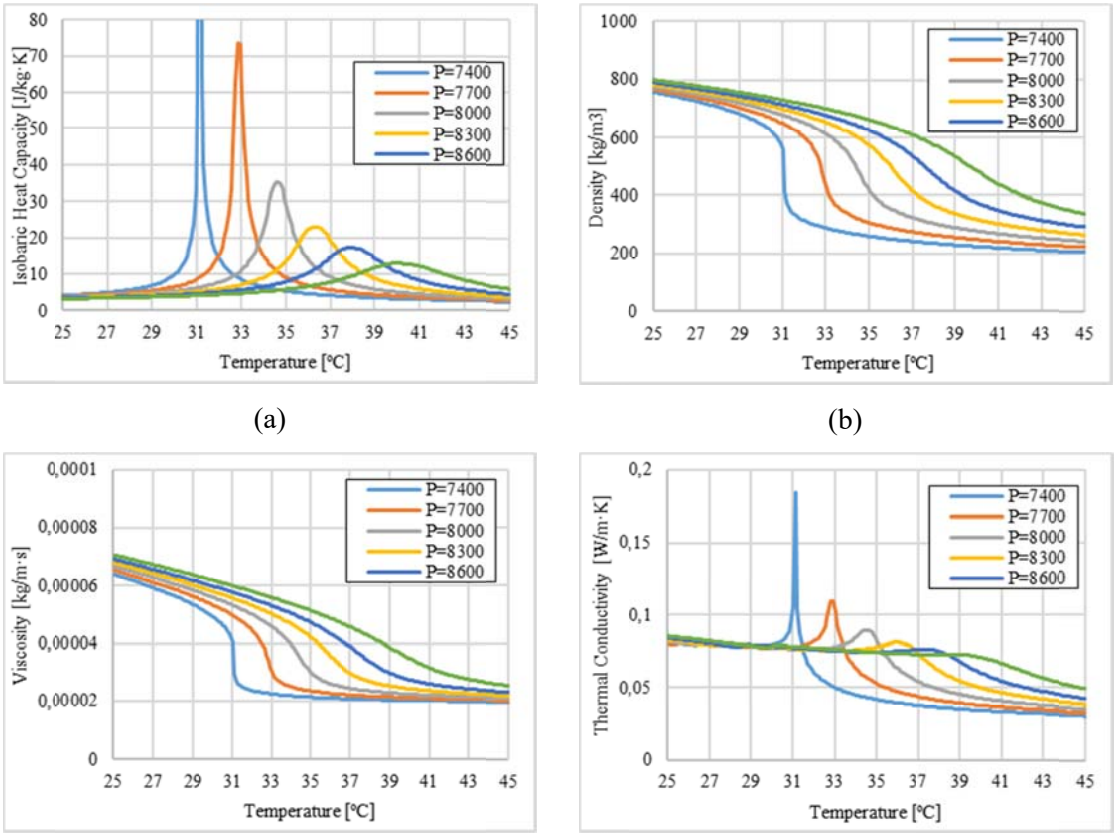

Figure 4. Properties of CO_2 vs temperature at different supercritical pressures: (a) heat capacity [35], (b) density [36], (c) thermal conductivity [38], and (d) dynamic viscosity [39].

4. Heat transfer improvement using supercritical CO_2

Many experimental data can be found in the literature, which led to empirical correlation for in-tube heat transfer of supercritical CO_2 [37]. In this chapter, the heat transfer characteristics of fluids at supercritical pressures and temperature will be introduced and the generated empirical correlations will be given. The experimental investigations will be presented for the cases of: horizontal tubes, vertical tubes, vertical packed bed tubes, vertical annulus, tube-in-tube, vertical natural circulation loop (NCL), channel configurations, micro-porous media, and some other configurations.

4.1. Heat transfer characteristics at supercritical pressures

The convection heat transfer of supercritical fluids in internal flow presents three major heat-transfer regimes [40]: normal, improved and deteriorated heat transfer. The deteriorated heat transfer usually appears at higher heat fluxes and lower mass fluxes and can be reduced significantly by increasing the level of turbulence [41]. The variations of the convective heat transfer are due to the dramatic variations of the thermophysical properties in radial direction, which lead to pseudo-boiling and pseudo-film boiling phenomena [42, 43].

The pseudo-boiling occurs when a supercritical fluid with a bulk temperature below its pseudocritical temperature (high density fluid) is heated from a surface, which results in a situation where some layers close to the wall are above pseudo-critical temperature. The low density fluid leaves the surface in the form of bubbles, improving the heat transfer regime. On the other hand, the pseudo-film boiling consists of a low density fluid preventing the contact to the surface of the high density fluid (bulk), limiting the heat transfer (deteriorated heat transfer regime).

Moreover, the variation of the thermophysical properties affects strongly the momentum and energy exchange and buoyant force change in the heat flux direction [44]. For instance, at a cooling surface, when there is a layer at pseudocritical temperature (between wall and bulk temperature), specific heat goes through a peak value with an increase in thermal conductivity which leads to a region of improved heat transfer [45].

According to Machida et al. [30], supercritical fluids have a larger compressibility and density compared to those of a gas which leads to unusual behaviour in their hydrodynamic and heat transfer properties. The transport phenomena of supercritical fluids has been reported by Carlès [46], who describes hydrodynamic and heat transfer mechanisms in terms of fluid relaxation, which is how the condition of a fluid changes according to perturbations in temperature, pressure or density. Among the mechanisms for relaxation of a supercritical fluid there is the piston effect, which is a thermal wave that moves through a compressible fluid causing expansion and compression of the hydrodynamic boundary layer (Figure 5). The piston effect plays a major role in the heat transfer of a supercritical fluid. Temperature perturbations are strongly affected by the piston effect; density perturbations are strongly affected by convection or diffusion effects; pressure perturbations are strongly affected by acoustical effects.

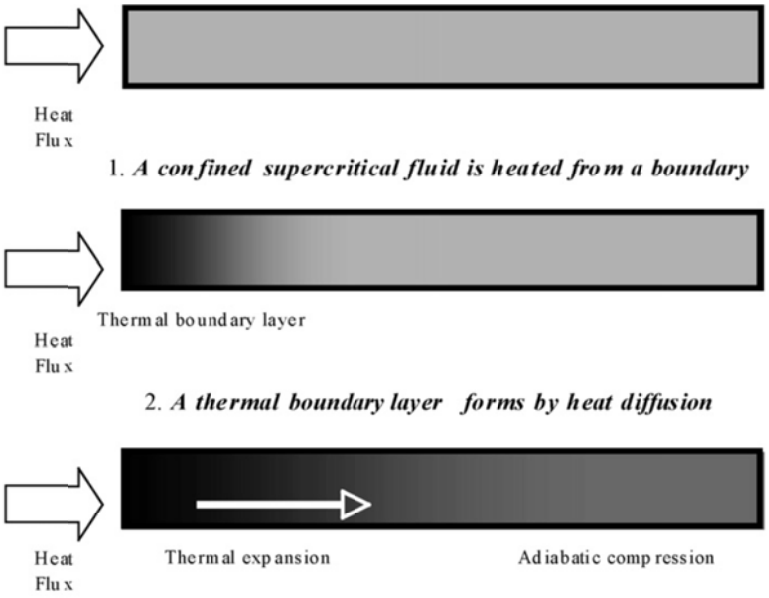

Figure 5. Qualitative description of the piston effect (grey scale represents temperature) [46].

The time scales for each of these phenomena is important. Diffusional and convectional relaxations have longer time-scales than the piston effect. Thus, density and temperature equilibration processes are usually decoupled for fluids in the supercritical region [46]. Zappoli et al. [47] proposed the piston effect as a major heat transport mechanism for supercritical fluids based on a one-dimensional Navier–Stokes equation and the van der Waals equation of state.

4.2. Nusselt correlations

The empirical correlations found in the literature were developed to take into account the great variations of the thermo physical properties under supercritical pressures, especially when bulk and wall temperature are significantly different (thermal gradient in the perpendicular direction of the flow) [49].

The first correlation that took into account this phenomenon was presented by Bringer and Smith [48], developed for vertical inner flows (Eq.1), considering Tx=Tb in case $\frac{T_{pc}-T_b}{T_w-T_b}<0$, and Tx=Tw if not.

$$Nu_b = 0.0375 \mathrm{Re}_x^{0.77} \mathrm{Pr}_w^{0.55} \qquad \text{(Eq.1)}$$

Krasnoshchekov et al. [50] (Eq.2-4) in 1969, developed a correlation for single horizontal tubes which was valid for a range of $9\cdot10^4 \leq Re_b \leq 3.2\cdot10^5$. This correlation was tested against the experimental data from Tanaka et al. [51] showing over-predictions around the pseudo-critical region. Within this context, Baskov et al. [52] developed in 1977 a correlation that reduced these over-predictions by 25% (Eq. 5) for the experimental range of $9.5\cdot10^4 \leq Re_b \leq 6.44\cdot10^5$. Moreover, Petrov and Popov [53] also reduces these over-predictions providing a correlation depending on the heat flux and mass flux, as shown in Eq. 6, which was valid for $3.1\cdot10^4 \leq Re_b \leq 8\cdot10^5$, $1.4\cdot10^4 \leq Re_w \leq 7.9\cdot10^5$, and $29 \leq q/G \leq 350$ J/kg. In addition, Fang et al. [54] extended the valid range of the previous correlation to $3000 \leq Re_w \leq 10^6$, $0 \leq q/G \leq 350$ J/kg (Eq. 7-10).

Krasnoshchekov et al. [49] correlation:

$$Nu_w = Nu_{iso,w}\left(\frac{\rho_w}{\rho_b}\right)^n\left(\frac{\bar{c}_p}{c_{p,w}}\right)^m \quad \text{(Eq. 2)}$$

where $Nu_{iso,w}$ was calculated as in Petukhov and Kirillov [55]

$$\bar{c}_p = \frac{h_b - h_w}{T_b - T_w} \quad \text{(Eq. 3)}$$

$$m = B\left(\frac{\bar{c}_p}{c_{p,w}}\right)^k \quad \text{(Eq. 4)}$$

where the coefficients n, B and k depend on pressure, as shown in Table 1.

Table 1. n, B and s constants for Krasnoshchekov et al. [50] equation.

Pressure (MPa)	8	10	12
n	0.38	0.68	0.8
B	0.75	0.97	1
k	0.18	0.04	0

Baskov et al. [52] correlation:

$$Nu_w = Nu_{iso,w}\left(\frac{\rho_b}{\rho_w}\right)^n\left(\frac{\bar{c}_p}{c_{p,w}}\right)^m \quad \text{(Eq. 5)}$$

if $T_b / T_{pc} \leq 1 \quad m = 1.4, n = 0.15$

The constants *n* and *m* are given in Table 2.

Table 2. *n* and *m* constants for Baskov et al. [45] equation.

	$\overline{c_p}/c_{p,w}>1$			$\overline{c_p}/c_{p,w}<1$		
P (MPa)	8	10	12	8	10	12
N	0.15	0.1	0	0.15	0.1	0
M	1.2	1.6	1.6	0.45	0.45	0.45

Petrov and Popov [53] correlation: $Nu_w = Nu_{iso,w}\left(1-0.001\frac{q}{G}\right)\left(\frac{\bar{c}_p}{c_{p,w}}\right)^n$ (Eq. 6)

$$n=\begin{cases}0.66-4\cdot10^{-4}\frac{q}{G}, when \frac{\bar{c}_p}{c_{p,w}}\le 1\\ 0.9-4\cdot10^{-4}\frac{q}{G}, when \frac{\bar{c}_p}{c_{p,w}}>1\end{cases}$$

Fang [54] correlation: $Nu_w = Nu_{o,w}\left(1-0.001\frac{q}{G}\right)\left(\frac{\bar{c}_p}{c_{p,w}}\right)^n$ (Eq. 7)

$$Nu_{o,w}=\frac{\left(f/8\right)(\mathrm{Re}_b-1000)\mathrm{Pr}_b}{A+12.7\sqrt{f/8}\left(\mathrm{Pr}_b^{2/3}-1\right)}$$ (Eq. 8)

$$f=8\left\{\left(\frac{8}{\mathrm{Re}}\right)^{12}+\left[\left(2.457\ln\frac{1}{\left(7/\mathrm{Re}\right)^{0.9}+0.27\varepsilon/D}\right)^{16}+\left(\frac{37530}{\mathrm{Re}}\right)^{16}\right]^{-1.5}\right\}^{1/12}$$ (Eq. 9)

$$A=\begin{cases}1+7\cdot10^{-8}\,\mathrm{Re}_w, when & \mathrm{Re}_w<10^6\\ 1.07, when & \mathrm{Re}_w\ge10^6\end{cases}$$ (Eq. 10)

Moreover, Pitla et al. [56] used an average value of Nusselt number (Eq. 11), evalutated at wall and bulk temperature using the correlation from Petukhov and Kirillov [57]. On the other hand, Yoon et al. [58] provided in 2003 a correlation (Eq. 12,13) based on pseudo-critical temperature, approach that was also used by Son and Park [59] (Eq. 14) and extended in 2010 by Oh and Son [60] for case of lower temperatures at the inlet (Eq. 15,16).

Pitla et al. [56] correlation: $Nu=\left(\frac{Nu_w+Nu_b}{2}\right)\frac{k_w}{k_b}$ (Eq. 11)

Yoon et al. [58] correlation: $Nu_b = 0.14\,\mathrm{Re}_b^{0.69}\,\mathrm{Pr}_b^{0.66}, when \quad T_b/T_{pc} > 1$ (Eq. 12)

$$Nu_b = 0.013\,\mathrm{Re}_b\,\mathrm{Pr}_b^{-0.05}\left(\frac{\rho_{pc}}{\rho_b}\right)^{1.6}, when \quad T_b/T_{pc} \le 1 \quad \text{(Eq. 13)}$$

Son and Park [59] correlation: $Nu_b = \mathrm{Re}_b^{0.55}\,\mathrm{Pr}_b^{0.23}\left(\frac{c_{p,b}}{c_{p,w}}\right)^{0.15}, when \quad T_b/T_{pc} > 1$ (Eq. 14)

$$Nu_b = \mathrm{Re}_b^{0.35}\,\mathrm{Pr}_b^{1.9}\left(\frac{\rho_b}{\rho_w}\right)^{-1.6}\left(\frac{c_{p,b}}{c_{p,w}}\right)^{-3.4}, when \quad T_b/T_{pc} \le 1$$

Oh and Son [60] correlation: $Nu_b = 0.023\mathrm{Re}_b^{0.7}\,\mathrm{Pr}_b^{2.5}\left(\frac{c_{p,b}}{c_{p,w}}\right)^{-3.5}, when \quad T_b/T_{pc} > 1$ (Eq. 15)

$$Nu_b = 0.023\,\mathrm{Re}_b^{0.6}\,\mathrm{Pr}_b^{3.2}\left(\frac{\rho_b}{\rho_w}\right)^{3.7}\left(\frac{c_{p,b}}{c_{p,w}}\right)^{-4.6}, when \quad T_b/T_{pc} \le 1 \text{ (Eq. 16)}$$

In recent years, several others correlations have been developed as function of ratios of thermophysical properties evaluated at wall and bulk temperature such as the ones reported by Jackson [61] (Eq. 17,18) for vertical tubes without buoyancy effects, Dang and Hibara [62] (Eq. 19) for horizontal tubes, Huai and Koyama [63] (Eq. 20), and Kuang et al. [64] (Eq. 21), last two focused on micro-channels. Moreover, similar approach has been used for the determination of Nusselt number in micro-fin tubes, as the one proposed by Lee et al. [65] (Eq. 22,23), or by Gupta et al. [66] (Eq. 24) for upward flows in tubes, or by Preda et al. [67] for horizontal and vertical tubes (Eq. 25), and recently by Saltanov et al. [68] (Eq. 26).

Jackson [61] correlation: $Nu_b = 0.0183\,\mathrm{Re}_b^{0.82}\,\mathrm{Pr}_b^{0.5}\left(\frac{\rho_w}{\rho_b}\right)^{0.3}\left(\frac{\overline{c_p}}{c_{p,b}}\right)^{n}$ (Eq. 17)

$$n = \begin{cases} 0.4 \quad when \quad T_b < T_w < T_{pc} \quad or \quad 1.2{\cdot}T_{pc} < T_b < T_w \\ 0.4 + 0.2\left(\frac{T_w}{T_{pc}} - 1\right) \quad when \quad T_b < T_{pc} < T_w \\ 0.4 + 0.2\left(\frac{T_w}{T_{pc}} - 1\right)\left[1 - 5\left(\frac{T_b}{T_{pc}} - 1\right)\right] \quad when \quad T_{pc} < T_b < 1.2T_{pc} \quad or \quad T_b < T_w \end{cases} \quad \text{(Eq. 18)}$$

Dang and Hibara [62] correlation: Same as Gnielinski, where Prandtl number is defined as:

$$\mathrm{Pr} = \begin{cases} c_{p,b}\mu_b / k_b, & when \quad c_{p,b} \geq \bar{c}_p \\ c_{p,}\mu_b / k_b, & when \quad c_{p,b} \geq \bar{c}_p \quad \& \quad \mu_b / k_b \geq \mu_f / k_f \\ c_{p,}\mu_f / k_f, & when \quad c_{p,b} \geq \bar{c}_p \quad \& \quad \mu_b / k_b < \mu_f / k_f \end{cases} \qquad \text{(Eq. 19)}$$

Huai and Koyama [63] correlation: $$Nu = 0.022186\,\mathrm{Re}^{0.8}\,\mathrm{Pr}^{0.3}\left(\frac{\rho_r}{\rho_w}\right)^{-1.4652}\left(\frac{\bar{c}_p}{c_{p,w}}\right)^{0.0832} \qquad \text{(Eq. 20)}$$

Kuang et al. [64] correlation: $$Nu = 0.001546\,\mathrm{Re}^{1.054}\,\mathrm{Pr}^{0.653}\left(\frac{\rho_w}{\rho}\right)^{0.367}\left(\frac{\bar{c}_p}{c_p}\right)^{0.4} \qquad \text{(Eq. 21)}$$

Lee et al. [65] correlation: $$Nu = \mathrm{Re}_b^{0.56}\,\mathrm{Pr}^{0.27}\left(\frac{c_{p,b}}{c_{p,w}}\right)^{0.2} \quad when \quad T_b / T_{pc} > 1 \qquad \text{(Eq. 22)}$$

$$Nu = \mathrm{Re}_b^{0.35}\,\mathrm{Pr}^{0.20}\left(\frac{c_{p,b}}{c_{p,w}}\right)^{-3} \quad when \quad T_b / T_{pc} \leq 1 \qquad \text{(Eq. 23)}$$

Gupta et al. [66] correlation $$Nu = 0.0038\,\mathrm{Re}_w^{0.957}\,\mathrm{Pr}_w^{0.139}\left(\frac{\mu_w}{\mu_b}\right)^{-0.222}\left(\frac{\rho_w}{\rho_b}\right)^{0.836}\left(\frac{k_w}{k_b}\right)^{-0.754} \qquad \text{(Eq. 24)}$$

Preda et al. [67] correlation $$Nu = 0.0015\,\mathrm{Re}_w^{1.03}\,\mathrm{Pr}_w^{0.76}\left(\frac{\mu_w}{\mu_b}\right)^{0.53}\left(\frac{\rho_w}{\rho_b}\right)^{0.46}\left(\frac{k_w}{k_b}\right)^{-0.43} \qquad \text{(Eq. 25)}$$

Saltanov et al. [68] correlation $$Nu = 0.0164\,\mathrm{Re}_b^{0.823}\,\mathrm{Pr}_b^{0.195}\left(\frac{\rho_w}{\rho_b}\right)^{0.374} \qquad \text{(Eq. 26)}$$

The effect of buoyancy has been found critical in the prediction of heat transfer coefficient. Therefore, Liao And Zhao [69] presented in 2002 a correlation (Eq. 27) to determine the Nusselt number of mini and micro channels as function not only of thermophysical properties evaluated at wall and bulk temperature but also on Grashof number (Eq. 28). Kim et al. [70] used similar approach for its application in vertical narrow annulus (Eq. 29-31), Simoes [71] for Kenics static mixer (Eq. 32), and Bruch et al. [72] for a vertical U-bend (Eq. 33).

Liao and Zhao [69] correlation: $$Nu_w = 0.128\,\mathrm{Re}_w^{0.8}\,\mathrm{Pr}_w^{0.3}\left(\frac{Gr}{\mathrm{Re}_b^2}\right)\left(\frac{\rho_b}{\rho_w}\right)^{0.437}\left(\frac{\bar{c}_p}{c_{p,w}}\right)^{0.411} \qquad \text{(Eq. 27)}$$

where Grashof number, defined as:

$$Gr = \frac{g(\rho_w - \rho_b)\rho_b D^3}{\mu_b^2} \qquad \text{(Eq. 28)}$$

Kim et al. [70] correlation: $$Nu_b = Nu_{\mathrm{var}} \cdot f(B) \qquad \text{(Eq. 29)}$$

$$f(B)=\begin{cases}\left(0.8+6\cdot10^{6}B\right)^{-0.8} & when \quad B\le 7\cdot10^{-8}\\ 0.261+3.068\cdot B^{0.1} & when \quad 7\cdot10^{-8}\le B\le 7\cdot10^{-7}\\ 1.47-6.7\cdot10^{5}\cdot B & when \quad 7\cdot10^{-7}\le B\le 10^{-6}\\ 0.8 & when \quad 10^{-6}\le B\le 10^{-5}\\ 0.1423\cdot B^{-0.15} & when \quad 10^{-5}\le B\end{cases} \quad \text{(Eq. 30)}$$

$$B=\frac{\overline{Gr}}{\mathrm{Re}_b^{2.7}\,\overline{\mathrm{Pr}}^{0.5}} \quad \text{(Eq. 31)}$$

Simões et al. [71] correlation:

$$Nu=0.558\,\mathrm{Re}_b^{0.8}\,\mathrm{Pr}_b^{0.4}\left(\frac{\rho_w}{\rho_b}\right)^{0.224}\left(\frac{\overline{c_p}}{c_{p,b}}\right)^{0.362}\left(\frac{Gr_b}{\mathrm{Re}_b^2}\right)^{0.07} \quad \text{(Eq. 32)}$$

Bruch et al. [72] correlation:

$$Nu=Nu_{FC}\cdot15\cdot\left(\frac{Gr_b}{\mathrm{Re}_b^{2.7}}\right)^{0.4} \quad \text{(Eq. 33)}$$

where, Nu_{FC} is the Nusselt number for pure force convection, calculated using the correlation proposed by Jackson (Eq. 17).

In 2012, Lin et al. [73] reviewed the existing correlations for Nusselt number of sCO_2 cooled in horizontal tubes, concluding that correlations provide higher accuracy when the heat flux is lower and hence buoyance is weaker. On the other hand, for cases where the buoyancy effect is stronger, all correlations fail in determining the heat transfer coefficient accurately.

4.3. Experimental investigations

Many researchers have pursued experimental investigations to determine the heat transfer properties of scCO2. A summary of those studies are presented in Table 3.

Table 3. Summary of experimental studies and their main findings.

Reference	**Geometry**	**Boundaries**	**Pressure**	**Main findings**
Walisch et al. [74]	10 mm di tube - Horizontal - Vertical - Inclined	30-180ºC	1-500 bar	- Heat transfer is affected by great variation of density and heat capacity for every studiedgeometry - The influence of density in Nusselt number, is dependent on Reynolds
Liao and Zhao [70]	Horizontal mini/micro circular tubes (diameters 0.5,0.7,1.1,1.4,1.55, and 2.16 mm)	20-110ºC	74-120 bar	- Up to Reynolds of $1 \cdot 10^5$Buoyancy effect was still significant, even though fluid was in forced motion - Comparison against previous correlations showing significant deviations - New correlation was developed
Pitla et al. [56]	Horizontal tube, diameter of 6.35 mm	20-124ºC	94- 134 bar	- Spike in the heat transfer coefficient in the pseudocritical region - New correlation was developed
Yoon et al. [59]	Horizontal tube, diameter of 7.73 mm	30-65ºC	75-88 bar	- Heat transfer coefficient increases near critical region -The increment of pressure near the pseudocritical temperature, decreases the heat transfer coefficient - Comparison against previous correlations showing significant deviations - Two new correlations were developed, modifying the one proposed by Baskov [52] and the one proposed by Dittus-Boelter [74].
Dand and Hihara [63]	Horizontal tube (diameters 1, 2 , 4, and 6 mm)	30-70ºC	80-100 bar	- Pressure drop and heat transfer coefficient increases with mass flux. - New correlation was developed based on the Gnielinski equation [75]
Son and Park [60]	Horizontal tube, diameter of	25-100ºC	75-100 bar	- Pressure drop during cooling process decreases as inlet pressure

	9.53 mm			increases - Comparison against previous correlations showing significant deviations - New correlation was developed
Oh and Son [61]	Horizontal tube (diameter 4.55 and 7.75 mm)	30-100 ºC	75-100 bar	- Smaller inner tube diameter showed higher heat transfer coefficient - Comparison against previous correlations showing significant deviations - New correlation was developed
Niu et al. [45] and Zhang et al. [77]	Horizontal tube, diameter of 18.4 mm	30-100 ºC	78-104 bar	- Tests were performed to investigate the characteristics of sCO2 in a solar collector in a solar energy powered Rankine cycle system (SRCS) - Apart from the variation of heat transfer around the critical point, it was measured that heat transfer can be enhanced significantly, by increasing the mass flow rate, reducing input heat flux and inlet pressure.
Tanimizu and Sadr [78]	Horizontal tube, diameter of 8.7 mm	16-64 kW/m^2	75-90 bar	- Wall temperature distribution shows a non-uniform variation due to severe fluid property change - Enhancement and deterioration of heat transfer coefficient was detected near the pseudocritical temperature
Jiant et al. [79]	Vertical tube, diameter 0.27 mm, upward and downward flows	96-550 kW/m^2	86 bar	- For Reynolds number higher than $4 \cdot 10^3$ the buoyancy and flow acceleration effects are significant both at low and high heat fluxes and upward and downward flows. - k- ε turbulence model provides the best results when Reynolds number is relatively high and heat flux is not very high

Jiang et al. [80]	Vertical tube, diameter 2 mm, upward and downward flows	4.5-13.7 kW/m^2	88 -120 bar	- The velocity distribution across the tubes developes as an M-shape when increaseing the heat flux, due to variation of physical properties and buoyancy. - For upward flow the transition between laminar and turbulent flow is identified and heat transfer is enhanced by the stron buoyancy. A clear dependance on the heat flux is observed in the heat transfer coefficient. -For downward flow the buoyancy enhanced the heat transfer coefficients along the entire tube, while for upward flow the buoyancy enhanced the heat transfer coefficients only in the latter part of the tube.
Mokry et al. [81]	Vertical tube, diameter 8 mm, upward flow	20-150 ºC	76-88 bar	- Deteriorated heat transfer was observed within the entrance region and near the middle of the test section - New correlation was developed
Jiang et al. [82]	Vertical micro tube, diameter 0.0992 mm, upward and downward flows	165-731 kW/m^2	88 bar	- The differences of Nusselt numbers between the upward and downward flows were small, which indicates that the buoyancy has little effect on the heat transfer in micro tubes - The local heat transfer increases continuously at low heat fluxes. - At higher heat fluxes, a non-linearity is observed in the heat transfer coefficient
Li et al. [83]	Vertical tube, diameter 2 mm, upward and downward flows	25-40ºC	78-95 bar	- A deterioration and recovery of the local heat transfer is found for upwards and downwards flows for high Reynolds number (Re>9000) and high heat fluxes - Comparison against previous correlations showing significant deviations, especially when buoyancy is significant

				- New correlation was developed
Kim and Kim [84]	Vertical tube, diameter 4.5 mm, upward flow	29-115ºC	75-103 bar	- The wall temperature is strongly influenced by wall heat flux and mass flux - The effect of flow acceleration and buoyancy on the Nusselt number is quantified - New correlation was developed and compared against experimental data from literature
Kim and Kim [85]	Vertical tube, diameter 4.5 mm, upward flow	29-115ºC	75-103 bar	- Flow acceleration and variation of the specific heat in the boundary layer influence drastically the heat transfer - A two layer (viscous sub-layer and buffer layer) heat transfer model has been developed to quantify the heat transfer of supercritical fluids - The developed two layer model provides an accuracy of ± 30%
Jiang et al. [86]	Vertical tube, inner diameter 4 mm, with porous media (particle diameter of 0.2-0.28 mm). Upward flow.	30-70ºC	95 bar	- When inlet temperature is higher than pseudocritical temperature, the heat transfer coefficient is lower than in the case where inlet temperature is lower than pseudocritical - At super-critical pressures, heat transfer coefficient is not always higher for larger mass flow rates - Heat transfer coefficients in porous tubes with low heat fluxes are much less than those with higher heat fluxes, which differs from the heat transfer in empty mini-tubes - In reduced heat flux conditions, heat transfer coefficient in porous tube is three times than that in the empty tube

Jiang et al. [87]	Vertical tube, inner diameter 4 mm, with porous media (particle diameter of 0.2-0.28 mm). Upward and downward flow.	30-70ºC	95 bar	- Supercritical Flow resistance in a porous tube is higher than the one predicted by the Aerov and Tojec correlation [88] - Two new correlations to predict friction factor in upward and downward flow are presented - The variation of heat capacity and buoyancy influences the convection heat transfer in the porous media
Jiang et al. [89]	Vertical tube, inner diameter 4 mm, with porous media (particle diameter of 0.2-0.28 mm). Upward and downward flow.	30-70ºC	95 bar	- In case inlet temperature is higher than pseudocritical temperature, the local heat transfer coefficient decrease uniformly through the porous vertical tube - In case inlet temperature is below the pseudocritical temperature, the local heat transfer coefficient have a maximum value when the fluid bulk temperature is near critical point - Effective thermal conductivity plays an important role in the convective heat transfer coefficient
Cho et al. [90]	Vertical annular channel, with inner diameter of 8 mm and outer of 10 mm	50-130 kW/m^2	81.2 bar	- The predicted heat transfer coefficient for the annular channel is larger than that for the tube - Three different turbulence models were compared against experimental data. SST k- ε and ABD (low Reynolds Abid) models are better than RNG k- ε model for the annular case.
Simões et al. [91]	Kenics static mixer, diameter of 4.623 mm, 21 helical mixing elements with length-to-diameter	10-50 ºC	80-210 bar	- Static mixer provided heat fluxes one order of magnitude higher than the ones obtained in tube-in-tube heat exchangers - A correlation of Nusselt number was developed.

	ratio of 1.7			
Kim et al. [70]	Vertical annular channel, with inner diameter of 8 mm and outer of 10 mm. Upward flow.	Up to 150 kW/m^2	77-82 bar	- At low mass flux, a deterioration of the heat transfer is found when heat flux is higher than 50 kW/m^2 - At higher mass flux, the deterioration of the heat transfer is lower and occurs at higher heat flux (150 kW/m^2) - A correlation of Nusselt number was developed.
Bruch et al. [73]	Vertical tube, inner diameter 6 mm. Upward and downward flow (U-bend)	15-70ºC	75-120 bar	- Heat transfer coefficient is maximum for a bulk temperature close to the pseudo-critical temperature - An increase of mass flux in upward flow leads to an increase of heat transfer coefficient. - In downward flows, there is a limit value of the mass flow rate below which a reduction leads to an enhancement of the heat transfer coefficient - Specific correlations were developed for upward and downward flows, with accuracy of 15% and 30%, respectively
Tokanai et al. [92]	Closed-loop circular pipe, inner diameters of 1.76, 4.35, or 10.1 mm.	50-80ºC	80-110 bar	- An empirical correlation was proposed for describing the heat transfer coefficient of sCO2 in a natural convection circulation system.
Chen et al. [93]	Closed-loop circular pipe, inner diameter 8 mm.	20-80ºC	60-150 bar	- The heating wall temperature has a greater effect on the Reynolds number in cooling pipe
Archana et al.[94]	Closed natural circular loop, inner diameter of 13.88 mm.	25 – 40ºC	85-95 bar	- 1D [95] based on empirical correlation and 2D [96] based on CFD numerical models were compared against experimental data. - Accuracy of 2D model is superior as it accounts for the developing

				flow effects.
Huai et al. [97]	Multi-port mini channels. 10 circular channels with inner diameter of 1.31 mm	22-53ºC	75-100 bar	- The pressure drop increases drastically with increasing the temperature in the region near the pseudocritical temperature - Enhanced and deteriorated heat transfer coefficient were also measured near the critical region - A new correlation was developed
Yun et al. [98]	Multi-port squared mini channels. 10 circular channels with hydraulic diameter of 1 mm	20-25 kW/m^2	84-104 bar	- The effect of oil on heat transfer coefficient of sCO_2 was tested in mini channels configuration - Significant degradation of average heat transfer coefficients were observed (20.4% with oil concentration 4 wt.%) - The degradation ratio of the heat transfer coefficient increases with increase of mass flux
Lee et al. [69]	Micro fin tube with an inner diameter of 4.6 mm	17-100ºC	80-100 bar	- The cooling heat transfer coefficient of the micro-fin tube increased by 12–39 % more than that of the smooth tube - Comparison against previous correlations showing significant deviations - New correlation was developed

5. Conclusions

$scCO_2$ is an interesting fluid for many applications, but the sharp variations of its thermophysical properties around the critical region lead to a unique heat transfer behaviour. Thus, standard heat transfer correlations cannot be used for the analysis of such systems. Therefore this review presents a summary of the applications where $scCO_2$ is being used or studied today, including chemical extraction in food science, pharmaceuticals, chemical residues, etc., extraction in petroleum refining and petrochemistry, separation processes in the food industry, in biotechnology, in extraction processes, and finally, as heat transfer fluid in power generation.

This review presents a comprehensive summary of all correlations available in literature to determine the heat transfer coefficient of $scCO_2$. Several authors have developed empirical correlations for specific geometries. Moreover, each of the correlations is developed for a given range of temperature, pressure, heat flux, and flow characteristics. Therefore, there is still a lack of a unique universal correlation applicable for a given geometry.

Finally, a summary of the experimental studies and their main findings available in the literature is shown. The used geometries are horizontal, vertical and inclined tubes, closed-loop circular pipes, and mini-channels with different dimensions and surface characteristics.

Acknowledgements

The work partially funded by the Spanish government (ENE2015-64117-C5-1-R (MINECO/FEDER) and ENE2015-64117-C5-3-R (MINECO/FEDER)). The authors would like to thank the Catalan Government for the quality accreditation given to their research group (2014 SGR 123). This project has received funding from the European Commission Seventh Framework Programme (FP/2007-2013) under Grant agreement NºPIRSES-GA-2013-610692 (INNOSTORAGE) and from the European Union's Horizon 2020 research and innovation programme under grant agreement No 657466 (INPATH-TES), and the funds received by the Royal Society of New Zealand. Alvaro de Gracia would like to thank Ministerio de Economia y Competitividad de España for Grant Juan de la Cierva, FJCI-2014-19940.

References

1. X Zhang, S Heinonen, E Levänen. Applications of supercritical carbon dioxide in materials processing and synthesis. RSC Advances 4 (2014) 61137-61152.
2. S Gupta, E Saltanov, SJ Mokry, I Pioro, L Trevani, D McGillivray. Developing empirical heat-transfer correlations for supercritical CO2 flowing in vertical bare tubes. Nuclear Engineering and Design 261 (2013) 116-131.
3. K Okamoto, J Ota, K Sakurai, H Madarame. Transient velocity distributions for the supercritical carbon dioxide forced convection heat transfer. Journal of Nuclear Science and Technology 40 (2003) 763-767.
4. BA Souza Machado , C Gambini Pereira , S Baptista Nunes , F Ferreira Padilha, MA Umsza-Guez Supercritical Fluid Extraction Using CO2: Main Applications and Future Perspectives, Separation Science and Technology 48 (2013) 2741-2760.
5. K Johns. Supercritical fluids – a novel approach to magnetic media production? Tribology International 31 (1998) 485-490.
6. MN Dadashev, GV Stepanov. Supercritical extraction in petroleum refining and petrochemistry. Chemistry and Technology of Fuels and Oils 36 (2000) 8-13.
7. M Raventós, S Duarte, R Alarcón. Application and Possibilities of Supercritical CO2 Extraction in Food Processing Industry: An Overview. Food Science and Technology International 8 (2002) 269-284.
8. F Sahena, ISM Zaidul, S Jinap, AA Karim, KA Abbas, NAN Norulaini, AKM Omar. Application of supercritical CO2 in lipid extraction – A review. Journal of Food Engineering 95 (2009) 240–253.
9. S Sarrade, C Guizard, GM Rios. New applications of supercritical fluids and supercritical fluids processes in separation. Separation and Purification Technology 32 (2003) 57-63.
10. SI Semenova, H Ohya, T Higashijima, Y Negishi. Separation of supercritical CO2 and ethanol mixtures with an asymmetric polyimide membrane. Journal of Membrane Science 74 (1992) 131-139.
11. JH Hsu, CS Tan. Separation of ethanol from aqueous solution by a method incorporating supercritical CO2 with reverse osmosis. Journal of Membrane Science 81 (1993) 273-285.
12. SV Dzyuba, RA Bartsch. Recent Advances in Applications of Room-Temperature Ionic Liquid/Supercritical CO2 Systems. Angewandte Chemie International Edition 42 (2003) 148-150.
13. K Khosravi-Darani, E Vasheghani-Farahani. Application of supercritical fluid extraction in biotechnology. Critical Reviews in Biotechnology 25 (2005) 231-242.

14. H Taher, S Al-Zuhair, A Al-Marzouqi, Y Haik, M Farid. Growth of microalgae using CO2 enriched air for biodiesel production in supercritical CO2. Renewable Energy 82 (2015) 61-70.
15. C Song. Global challenges and strategies for control, conversion and utilization of CO2 for sustainable development involving energy, catalysis, adsorption and chemical processing. Catalysis Today 115 (2006) 2–32.
16. M Sauceu, J Fages, A Common, C Nikitine, E Rodier. New challenges in polymer foaming: A review of extrusion processes assisted by supercritical carbon dioxide. Progress in Polymer Science 36 (2011) 749–766.
17. J Eastoe, C Yan, A Mohamed. Microemulsions with CO2 as a solvent. Current Opinion in Colloid & Interface Science 17 (2012) 266–273.
18. GC Glatzmaier, CS Turchi. Supercritical CO2 as a heat transfer and power cycle fluid for CSP systems. ASME International Conference on Energy Sustainability, Proceedings, 3rd, San Francisco, CA, United States, July 19-23, 2009, 2, 673-676.
19. G Manente, A Lazzaretto. Innovative biomass to power conversion systems based on cascaded supercritical CO2 Brayton cycles. Biomass and Bioenergy 69 (2014) 155-168.
20. L Hu, D Chen, Y Huang, L Li, Y Cao, D Yuan, J Wang, L Pan. Investigation on the performance of the supercritical Brayton cycle with CO2-based binary mixture as working fluid for an energy transportation system of a nuclear reactor. Energy 89 (2015) 874–886.
21. JI Linares, LE Herranz, I Fernandez, A Cantizano, BY Moratilla. Supercritical CO2 Brayton power cycles for DEMO fusion reactor based on Helium Cooled Lithium Lead blanket. Applied Thermal Engineering 76 (2015) 123-133.
22. H Yamaguchi, XR Zhang, N Sawada, H Suzuki, H Ueda. Experimental study on a solar water heater using supercritical carbon dioxide as working fluid. ASME International Conference on Energy Sustainability, Proceedings, 3rd, San Francisco, CA, United States, July 19-23, 2009, 2, 753-759.
23. JC Hsieh, DTW Lin, CH Wei, HJ Huang. The Heat Extraction Investigation of Supercritical Carbon Dioxide Flow in Heated Porous Media. Energy Procedia 61 (2014) 262-265.
24. L Zhang, F Luo, R Xu, P Jiang, H Liu. Heat Transfer and Fluid Transport of Supercritical CO2 in Enhanced Geothermal System with Local Thermal Non-equilibrium Model. Energy Procedia 63 (2014) 7644-7650.
25. V Dostal, MJ Driscoll, P Hejzlar. A supercritical carbon dioxide cycle for next generation nuclear reactors. [Dissertation] Massachusetts Institute of Technology, Cambridge (MA) (2004 Jan), p. 317 Report No.: MIT-ANP-TR-100
26. Z Ma, CS Turchi. Advanced supercritical carbon dioxide power cycle configurations for use in concentrating solar power systems. S. Wright, R. Linden, M. Anderson (Eds.), Supercritical CO2 Power Cycle Symposium; May 24-25; Boulder, CO (USA) (2011)

27. GA Johnson, MW McDowell. Supercritical CO2 cycle development at Pratt & Whitney Rocketdyne. S. Wright, R. Linden, M. Anderson (Eds.), Supercritical CO2 Power Cycle Symposium; May 24-25; Boulder, CO (USA) (2011).
28. SA Wright, RF Radel, ME Vernon, GE Rochau, PS Pickard. Operation and analysis of a supercritical CO2 Brayton cycle. Albuquerque, New Mexico, USA (2010) Sandia Report, No SAND2010e0171. Available from: prod.sandia.gov/techlib/access-control.cgi/2010/100171.pdf
29. A Cavallini, D Del Col, L Rossetto. Heat transfer and pressure drop of natural refrigerants in minichannels (low charge equipment). International Journal of Refrigeration 36 (2013) 287-300.
30. H Machida, M Takesue, RL Smith. Green chemical processes with supercritical fluids: Properties, materials, separations and energy. Journal of Supercritical Fluids 60 (2011) 2-15.
31. B Zalba, JM Marín, LF Cabeza, H Mehling. Review on thermal energy storage with phase change materials: Materials, heat transfer analysis and applications. Applied Thermal Engineering 23 (2003) 251-283.
32. MM Farid, AM Khudhair, SAK Raack, S Al-Hallaj. A review on phase change energy storage: Materials and Applications. Energy conversion and management 45 (2004) 1597-1615.
33. BT Swapnalee, PK Vijayan, M Sharma, DS Pilkhwal. Steady state flow and static instability of supercritical natural circulation loops. Nuclear Engineering and Design 245 (2012) 99-112.
34. M Sharma, PK Vijayan, DS Pilkhwal, Y Asako. Steady state and stability characteristics of natural circulation loops operating with carbon dioxide at supercritical pressures for open and closed loop boundary conditions. Nuclear Engineering and Design 265 (2013) 737-754.
35. BL Koppel, JM Smith. Thermal properties of carbon dioxide in the critical region. Journal of Chemical & Engineering Data 5 (1960) 437-440.
36. R Span, W Wagner. A new equation of state for carbon dioxide covering the fluid region from the triple-point temperature to 110 K at pressures up to 800 MPa. J. Chem. Eng. Data 25 (1996) 1509.
37. P Surendran, S Gupta, T Preda, I Pioro. Comparison of existing supercritical carbon dioxide heat transfer correlations for horizontal and vertical bare tubes. Proceedings of the 20th International Conference on Nuclear Engineering collocated with ASME Power Conference (2012), Anaheim, USA, 8 pages.
38. V Vesovic, WA Wakeham. The transport properties of carbon dioxide. Journal of Chemical and Engineering Data 19 (1990) 763-808.

39. A Fenghour, WA Wakeham, V Vesovic. The viscosity of carbon dioxide. Journal of Physical and Chemical Reference Data 27 (1998) 31-44.
40. A Belmiloudi. Heat transfer – Theoretical Analsysis, Experimental investigations and industrial systems (2011), chapter 22.
41. RB Duffey, IL Pioro. Experimental heat transfer of supercritical carbon dioxide flowing inside channels (survey). Nuclear Engineering and Design 235 (2005) 913-924.
42. I Pioro, S Mokry. Thermophysical Properties at Critical and Supercritical Conditions, in "Heat Transfer. Theoretical Analysis, Experimental Investigations and Industrial Systems", (2011) INTECH, Rijeka, Croatia, pp. 573-592.
43. I Pioro, S Mokry. Heat transfer to Fluids at supercritical pressures, in "Heat Transfer. Theoretical Analysis, Experimental Investigations and Industrial Systems", (2011) INTECH, Rijeka, Croatia, pp. 481-504.
44. J Yang, Y Ma, S Liu, X Zeng. Comparison investigation on the heat transfer characteristics for supercritical CO2 fluid and conventional refrigerants. 7th IIR Gustav Lorentzen Conference on Natural Working Fluids, Trondheim, Norway, May 28-31, 2006.
45. X Niu, H Yamaguchi, X Zhang, Y Iwamoto, N Hashitani. Experimental study of heat transfer characteristics of supercritical CO2 fluid in collectors of solar Rankine cycle system. Applied Thermal Engineering 31 (2011) 1279-1285.
46. P Carles. A brief review of the thermophysical properties of supercritical fluids. Journal of Supercritical Fluids 53 (2010) 2-11.
47. B Zappoli, D Bailly, Y Garrabos, B Le Neindre, P Guenoun, D Beysens. Anomalous heat transport by the piston effect in supercritical fluids under zero gravity. Physical Review A: Atomic, Molecular, and Optical Physics 41 (1990) 2264-2267.
48. RP Bringer, JM Smith. Heat transfer in the critical region, AIChE Journal 3 (1957) 49-55.
49. X Fan, Y Xu. Modified heat transfer equation for in-tube supercritical CO2 cooling. Applied Thermal Engineering 31 (2011) 3036-3042.
50. EA Krasnoshchekov, IV Kuraeva, VS Protopopov. Local heat transfer of carbon dioxide under supercritical pressure under cooling conditions. Teplofizika Bysokikh Temperatur 7 (1969) 922-930.
51. H Tanaka, N Nishiwaki, M Hirata. Turbulent heat transfer to supercritical carbon dioxide. Semi-International Symposium. Japan Society of Mechanical Engineers, Tokyo, Japan, 1967.
52. VL Baskov, IV Kuraeva, VS Protopopov. Heat transfer with the turbulent flow of a liquid under supercritical pressure in tubes under cooling conditions. High Temperature 15 (1977) 81-86.
53. NE Petrov, VN Popov. Heat transfer and resistance of carbon dioxide being cooled in the supercritical region. Thermal Engineering 32 (1985) 131-134.

54. XD Fang. Modeling and analysis of gas coolers. ACRC CR-16. Department of Mechanical and Industrial Engineering, University of Illinois at Urbana-Champaing, USA, 1999.
55. BS Petukhov, VN Popov. Theoretical calculation of heat exchange and frictional resistance in turbulent flow in tubes of an incompressible fluid with thermophysical properties. High Temperature 1 (1963) 69-83.
56. SS Pitla, EA Groll, S Ramadhyani. New correlation to predict the heat transfer coefficient during in-tube cooling of turbulent supercritical CO2. International Journal of Refrigeration 25 (2002) 887-895.
57. BS Petukhov, VV Kirillov. On heat exchange at turbulent flow of liquid in pipes. Teploenergetika 4 (1958) 63-68.
58. SH Yoon, JH Kim, YW Hwang, MS Kim, K Min, Y Kim. Heat transfer and pressure drop characteristics during the in-tube cooling process of carbon dioxide in the supercritical region. International Journal of Refrigeration 26 (2003) 857-864.
59. CH Son, SJ Park. An experimental study on heat transfer and pressure drop characteristics of carbon dioxide during gas cooling process in a horizontal tube. International Journal of Refrigeration 29 (2006) 539-546.
60. HK Oh, CH Son. New correlation to predict the that transfer coefficient in-tube cooling of supercritrical CO2 in horizontal macro-tubes. Experimental Thermal and Fluid Science 34 (2010) 1230-1241.
61. JD Jackson. Consideration of the heat transfer peroperties of supercritical pressure water in connection with the cooling of advanced nuclear reactors, Proceedings of the 13th Pacific Basin Nuclear Conference, Shenzhen City, Shina, October 21-25, 2002.
62. C Dang, E Hibara. In-tube cooling heat transfer of supecritical carbon dioxide. Part 1. Experimental measurement. International Journal of Refrigeration 27 (2007) 736-747.
63. XL Huai, S Koyama. Heat transfer characteristics of supercritical CO2 flow in small-channeled structures. Experimental Heat Transfer 20 (2007) 19-33.
64. G Kuang, M Ohadi, S Dessiatoun. Semi-empirical correlation of gas cooling heat transfer of supercritical carbon dioxide in microchannels. HVAC & R Research 16 (6) (2008) 861-871.
65. H Lee, H Kim, J Yoon, K Choi, C Son. The cooling heat transfer characteristics of the supercritical CO2 in micro-fin tube. Heat and Mass Transfer 49 (2013) 173-184.
66. S Gupta, D McGillivray, P Surendran, L Trevani, I Pioro. Developing heat-transfer correlations for supercritical CO2 flowing in vertical bare tubes. Proceedings of the 20th International Conference on Nuclear Engineering collocated with ASME Power Conference (2012), Anaheim, USA, 13 pages.
67. T Preda, E Saltanov, K Gabriel, I Pioro. Development of a heat transfer correlation for supercritical CO2 based on multiple data sets. Proceedings of the 20th International

Conference on Nuclear Engineering collocated with ASME Power Conference (2012), Anaheim, USA, 7 pages.

68. E Saltanov, I Pioro, D Mann, S Gupta, S Mokry, G Harvel. Study on specifics of forced-convective heat transfer in supercritical carbon dioxide. Journal of Nuclear Engineering and Radiation Science 1 (2015) 1–8.
69. SM Liao, TS Zhao. Measurement of heat transfer coefficient from supercritical carbon dioxide flowing in horizontal mini/micro channels. Journal of Heat Transfer 124 (2002) 413-420
70. HY Kim, Y Kim, DJ Kang, JH Song, YY Bae. Experimental investigations on heat transfer to CO2 flowing upward in a narrow annulus at supercritical pressures. Nuclear Engineering and Technology 40 (2007) 155-162
71. P Simões, B Afonso, J Fernandes, JPB Mota. Static mixers as heat exchangers in supercritical fluid extraction processes. Journal of Supercritical Fluids 43 (2008) 477-483
72. A Bruch, A Bontemps, S Colasson. Experimental investigation of heat transfer of supercritical carbon dioxide flowing in a cooled vertical tube. International Journal of Heat and Mass Transfer 52 (2009) 2589-2598
73. W Lin, Z Du, A Gu. Analysis of heat transfer correlations of supercritical CO2 cooled in horizontal circular tubes. Heat and Mass Transfer 48 (2012) 705-711.
74. T Walisch, M Müller, W Döfler, C Trepp. The heat transfer to supercritical carbon dioxide in tubes with mixed convection. Process Technology Proceedings 12 (1996) 199-204
75. FW Dittus, LMK Boelter. Heat transfer in automobile radiators of the tubular type. University of California Publications of Engineering 2 (1930) 443–461.
76. V Gnielinski. New equations for heat and mass transfer in turbulent pipe and channel flow. International Journal of Chemical Engineering 16 (1976) 359 –368.
77. Z Zhang, H Yamaguchi. An experimental investigation on characteristics of supercritical CO2-based solar Rankine system. International Journal of Energy Research 35 (2011) 1168-1178.
78. K Tanimizu, R Sadr. Experimental investigation of buoyancy effects on convection heat transfer of supercritical CO2 flow in a horizontal tube. Heat and Mass Transfer 52 (2016) 713-726.
79. P Jiang, Y Zhang, R Shi. Experimental and numerical investigation of convection heat transfer of CO2 at supercritical pressures in a vertical mini tube. International Journal of Heat and Mass Transfer 51 (2008) 3052–3056.
80. P Jiang, Y Zhang, Y Xu, R Shi. Experimental and numerical investigation of convection heat transfer of CO2 at supercritical pressures in a vertical tube at low Reynolds numbers. International Journal of Thermal Sciences 47 (2008) 998-1011.

81. S Mokry, IL Pioro, B Duffey. Experimental heat transfer to supercritical CO2 flowing upward in a bare vertical tube. Proceedings of SCCO2 Power Cycle symposium 2009.
82. P Jiang, R Xu, Z Li, C Zhao. Influence of flow acceleration on convection heat transfer of CO2 at supercritical pressures and air in a vertical micro tube. Proceedings of the 14th International Heat Transfer Conference, Washington, 2010.
83. Z Li, P Jiang, C Zhao, Y Zhang. Experimental investigation of convection heat transfer of CO2 at supercritical pressures in a vertical circular tube. Experimental Thermal and Fluid Science 34 (2010) 1162-1171.
84. DE Kim, MH Kim. Experimental study of the effects of flow acceleration and buoyancy on heat transfer in a supercritical fluid flow in a circular tube. Nuclear Engineering and Design 240 (2010) 3336-3349
85. DE Kim, MH Kim. Two layer heat transfer model for supercritical fluid flow in a vertical tube. The Journal of Supercritical Fluids 58 (2011) 15-25.
86. P Jiang, Y Xu, J Lv, R Shi, S He, JD Jackson. Experimental investigation of convection heat transfer of CO2 at super-critical pressures in vertical mini-tubes and in porous media. Applied Thermal Engineering 24 (2004) 1255-1270
87. P Jiang, R Shi, Y Xu, S He, JD Jackson. Experimental investigation of flow resistance and convection heat transfer of CO2 at supercritical pressures in a vertical porous tube. The Journal of Supercritical Fluids 38 (2006) 339-346.
88. ME Aerov, OM Tojec, Hydraulic and Thermal Basis on the Performance of Apparatus with Stationary and Boiling Granular Layer, Himia Press, Leningrad, 1968 (in Russian).
89. P Jiang, R Shi, C Zhao, Y Xu. Experimental and numerical study of convection heat transfer of CO2 at supercritical pressures in vertical porous tubes. International Journal of Heat and Mass Transfer 51 (2008) 6283–6293
90. B Cho, Y Kim, Y Bae. Prediction of a heat transfer to CO2 flowing in an upward path at a supercritical pressure. Nuclear Engineering and Technology 41 (2009) 907-920.
91. P Simões, B Afonso, J Fernandes, JPB Mota. Static mixers as heat exchangers in supercritical fluid extraction processes. Journal of Supercritical Fluids 43 (2008) 477-483.
92. H Tokanai, Y Ohtomo, H Horiguchi, E Harada, M Kuriyama. Heat transfer of supercritical CO2 flow in natural convection circulation system. Heat Transfer Engineering, 31 (2010) 750-756.
93. L Chen, B Deng, X Zhang. Experimental investigation of CO2 thermosyphon flow and heat transfer in the supercritical region. International Journal of Heat and Mass Transfer 64 (2013) 202-211.
94. V. Archana, A.M. Vaidyia, P.K. Vijayan. Numerical modeling of supercritical CO2 natural circulation loop. Nuclear engineering and design 293 (2015) 330-345.

95. V. Archana, A.M. Vaidyia, P.K. Vijayan. Flow transients in Supercritical CO2 natural circulation loop. Procedia Engineering 127 (2015) 1189-1196.
96. V. Archana, A.M. Vaidyia, P.K. Vijayan. Effect of Pressure on steady state and heat transfer characteristics in supercritical CO2 natural circulation loop. Procedia Engineering 127 (2015) 636-644.
97. XL Huai, S Koyama, TS Zhao. An experimental study of flow and heat transfer of supercritical carbon dioxide in multi-port mini channels under cooling conditions. Chemical Engineering Science 60 (2005) 3337-3345.
98. R Yun, Y Hwang, R Radermacher. Convective gas fooling heat transfer and pressure drop characteristics of supercritical CO2/oil mixture in a minichannel tube. International Journal of Heat and Mass Transfer 50 (2007) 4796-4804.